Eur. Phys. J. B **15**, 235–246 (2000)

THE EUROPEAN PHYSICAL JOURNAL B

EDP Sciences

Structural transformation from the AlCuFe icosahedral phase to the 1/1 cubic α(AlSi)CuFe approximant phase; three dimensional models of translation defects

A. Le Lann and J. Devaud

Centre d'Études de Chimie Métallurgique – CNRS, 15 rue Georges Urbain 94407 Vitry sur Seine Cedex, France

Received 31 May 1999 and Received in final form 23 December 1999

Abstract. Unusual results are obtained by High Resolution Electron Microscopy (HREM) studies of the 1/1 cubic approximant phase of the (AlSi)CuFe icosahedral phase. We study, in a 3D model of AlCuFe icosahedral phase, the possibilities of transformation of this structure into a periodic cubic structure. We propose a model of transformation coherent with the experimental results.

PACS. 61.64.Br Quasicrystals

1 Introduction

A 1/1 cubic approximant phase has been synthesized by substituting a few percent of Si for Al in the canonical $Al_{62}Cu_{25.5}Fe_{12.5}$ icosahedral phase. The $Al_{55}Si_7Cu_{25.5}Fe_{12.5}$ phase, denoted α phase, is obtained, almost without change in the chemical composition, by annealing for 2 hours at 750 °C the as-quenched (AlSi)CuFe icosahedral phase; its parameter is $a_\alpha = 1.233$ nm. The X-ray powder diffraction pattern reveals a high structural quality; it is in good agreement with the calculated diagram for the p/q = 1/1 cubic approximant. The kinetic of the transformation from the as-quenched icosahedral structure (obtained as flakes) to the 1/1 cubic structure is considerably faster than in the case of the other AlCuFe approximants: typically, in the same range of temperatures, 2 to 3 hours of annealing treatment instead of several days [1].

We present (Sect. 2) experimental results obtained on this new phase by High Resolution Electron Microscopy (HREM). The HREM study confirms the cubic periodicity of the structure over large areas, but reveals the presence of translation defects; the translation vectors, determined by geometric phase analysis [2], are not rational vectors of the cubic structure.

In the theoretical models (calculated by 6D → 3D projection) of the transformation from icosahedral to approximant structure, it is assumed *a priori* that the approximant phase is a periodic arrangement of identical cells, as in any crystalline structure. In the case of a cell as small as the 1/1 cubic cell, such a model implies the whole reconstruction of the structure. The (AlSi)CuFe icosahedral phase contains very stable clusters (Bergman clusters Sect. 3.1) and the rapidity of its transformation into the 1/1 cubic α (AlSi)CuFe phase seems to be incompatible with a process of nucleation and growth.

The unusual results obtained by the HREM study lead us to propose another hypothesis: the 1/1 cubic approximant structure could result from the assemblage of small domains containing a few cubic cells which can be identified everywhere in the perfect icosahedral structure.

We describe these domains in a three-dimensional (3D) model of the AlCuFe icosahedral structure [3–5], and we identify the different translation vectors between them (Sects. 3.1 and 3.2).

In Sections 3.3 and 3.4, the experimental results obtained by HREM and geometric phase analysis are compared to different assemblages of domains.

In Section 3.5, we describe structural models for the transformation of the icosahedral phase into the 1/1 cubic structure, which results from the best assemblages of domains: in such cases, the translation vectors between the domains correspond to the smallest distance between atoms in the icosahedral structure.

2 Experimental results

2.1 HREM study

In the $Al_{55}Si_7Cu_{25.5}Fe_{12.5}$ α phase, annealed for 2 hours at 750 °C, large grains (several microns) separated by smooth boundaries are observed; the bright field contrast is uniform and there are very few defects (Fig. 1a). The density of defects is much higher in the $Al_{57}Si_5Cu_{27}Fe_{11}$ phase, denoted α_1 phase [6] (Fig. 1b). These defects are translation defects (see Sects. 2.2 and 3.4) which do not disappear with annealing treatment. The comparison of Figures 1a

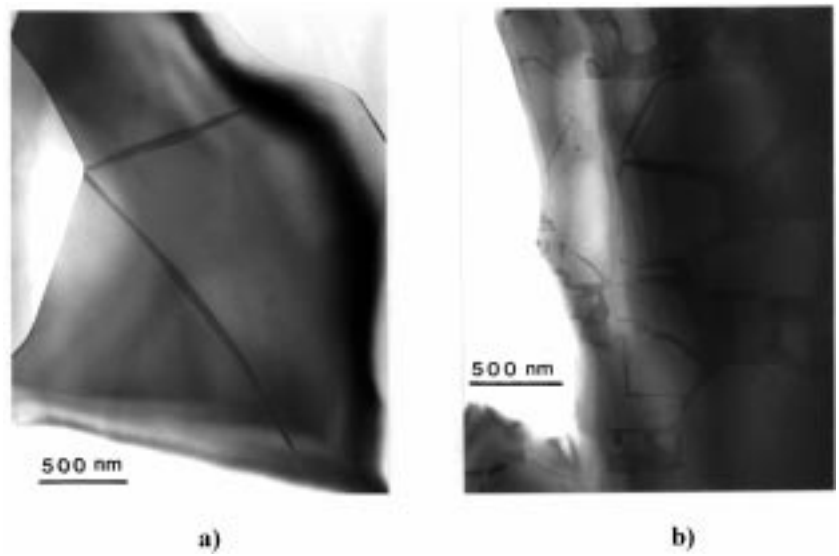

Fig. 1. (a) Perfection of the $Al_{55}Si_7Cu_{25.5}Fe_{12.5}$ α phase, annealed for 2 hours at 750 °C. (b) Density of translation defects in the $Al_{57}Si_5Cu_{27}Fe_{11}$ α_1 phase, annealed for 48 hours at 650 °C.

and 1b shows that the characteristics of these phases are very dependent on their chemical composition.

A cubic periodicity over large areas of the α structure appears on the HREM images along $\langle 100 \rangle$ and on the diffraction pattern (Figs. 2a–2d). There is no evidence for a centre of symmetry within the cell.

The contrast observed in Figure 2b is the most frequently observed in the cubic approximant structure: all the traces of planes belong to the cubic system. However, it can be found, within the same sample, a different contrast (Figs. 2c and 2d): diffuse portions of traces of planes are visible; their irrational orientation coincides with five-fold planes of the "parent" icosahedral phase.

2.2 Translation defects

Translation defects separating large areas of perfect cubic structure are observed in the α(AlSi)CuFe phase. Their habit planes are frequently either {100} or {110} cubic planes (Fig. 1b). We have already presented [7], the measure by geometric phase analysis of the translation vectors between different domains. In all cases, the translations measured in the observation plane are irrational fractions of the cubic parameter. In the case of three defects meeting at a triple junction [8], the translation vectors were identified as vectors of the icosahedral phase.

3 Three dimensional (3D) model of structural transformation from the icosahedral to the cubic approximant phase

3.1 Structural model of the AlCuFe 1/1 cubic approximant cell

A 3D model of the AlCuFe icosahedral structure has been obtained by irrational projection in parallel space (3D real space) of the nodes of a 6D hypercubic lattice [3,4,9]. It was determined from a 6D neutron diffraction study [10] that the AlCuFe icosahedral structure is defined in 6D space by 3 atomic surfaces located at the N [000000] and N′ [100000] nodes of a primitive lattice and at the BC 1/2[111111] body-centre; the other BC′ 1/2[11111$\overline{1}$] body-centre is vacant. The size and shape of the atomic surfaces, in perpendicular space, determine the occupation in real space of the nodes of the four sublattices:

$$\mathrm{I} = \mathrm{P}_1 \oplus \mathrm{P}_2 = (\mathrm{N} \oplus \mathrm{N}') \oplus (\mathrm{BC} \oplus \mathrm{BC}').$$

Figure 3 is a two-fold section of this 3D model, previously described by Le Lann and Devaud [5]. The BC node located at the centre of this limited volume of icosahedral structure is taken as the origin of coordinates. Five sets of three orthogonal two-fold planes intersect at the origin ($x = y = z = 0$); we select one set of orthogonal two-fold planes perpendicular to the x, y and z axes; they are mirror planes of this portion of the icosahedral structure. Five-fold and three-fold planes are perpendicular to the A_5 and A_3 axes. Each two-fold axis bears nodes belonging to only one sublattice [11]; this allows a simple description of the cubic cells.

Any AlCuFe approximant structure results from a rational projection, in real space, of the AlCuFe (6D) structure. Both icosahedral and approximant structures have in common a volume of icosahedral structure that can be larger than the periodic cell [8,12]. It results from these constructions that a 3D model for the AlCuFe 1/1 cubic approximant cell is necessarily a cube taken out of the 3D model of the AlCuFe icosahedral structure.

Different models of this cell are presented on two-fold sections of the icosahedral model (Figs. 4 and 5); in all cases the $\langle 100 \rangle$ edges of the approximant cell are parallel to one of the 5 sets of orthogonal two-fold axes of the icosahedral structure. The edge length is $a_\alpha = a_{\mathrm{ico}}\sqrt{(8+12\tau)/(2+\tau)} = 1.229$ nm in the AlCuFe model

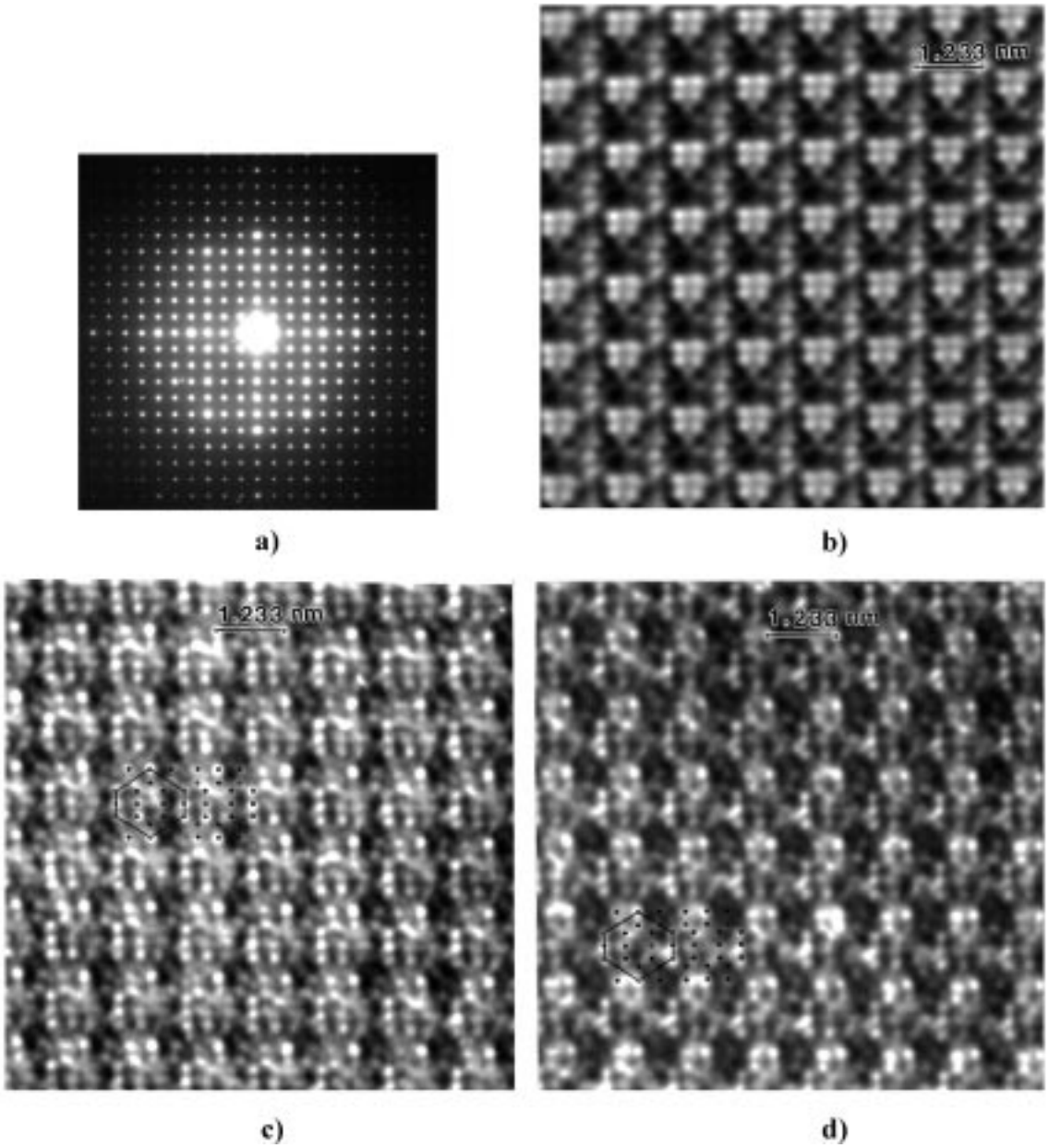

Fig. 2. ⟨100⟩ HREM images of the $Al_{55}Si_7Cu_{25.5}Fe_{12.5}$ α cubic approximant phase; the three images have been obtained on the same sample. (a) Corresponding diffraction pattern. (b) All the traces of planes belong to the cubic system. (c) The diffuse portions of traces of planes coincide with the orientation of five-fold planes of the icosahedral structure. The contrast observed within the cell can be identified with the two-fold projection of the nodes of a triacontahedron (as in Fig. 8c): the N nodes of the dodecahedron are shown by white circles and the N′ nodes of the icosahedron, by black circles. (d) In the same photographic plate, at a distance of only 20 nm from Figure 2c, strong dots form a "square" group whose relative intensities vary from one cell to the next.

where $a_{\rm ico} = 0.4465$ nm. Two sections of the cells are represented, one in the plane $z = 0$, the other in the plane $z = \pm a_{\rm ico}\sqrt{(2+3\tau)/(2+\tau)} = \pm 1/2a_\alpha$. (In order to get simpler values for the coordinates of the icosahedral planes, we approximate the edge length by $a_\alpha = 1.228$ nm that corresponds to $a_{\rm ico} = 0.446$ nm.)

Figure 4a, in the plane $z = 0$, represents the face of a cell constructed on BC vertices, whose midsection (BC′ centre) is drawn in the plane $z = \pm 1/2a_\alpha$ (Fig. 4b). And reciprocally, Figure 4b represents the face of a cell constructed on BC′ vertices whose midsection (BC centre) is shown in Figure 4a.

In these cells, the N and N′ nodes are the projections of the 64 nodes of a 6D unit cell belonging to P_1: 32 nodes form a triacontahedron inscribed in the cubic cell (icosahedron of radius $\tau a_{\rm ico}$ on N′ nodes, and dodecahedron of radius $0.910\tau a_{\rm ico}$ on N nodes in Fig. 4a and reciprocally in Fig. 4b); inside the cell, 32 nodes correspond

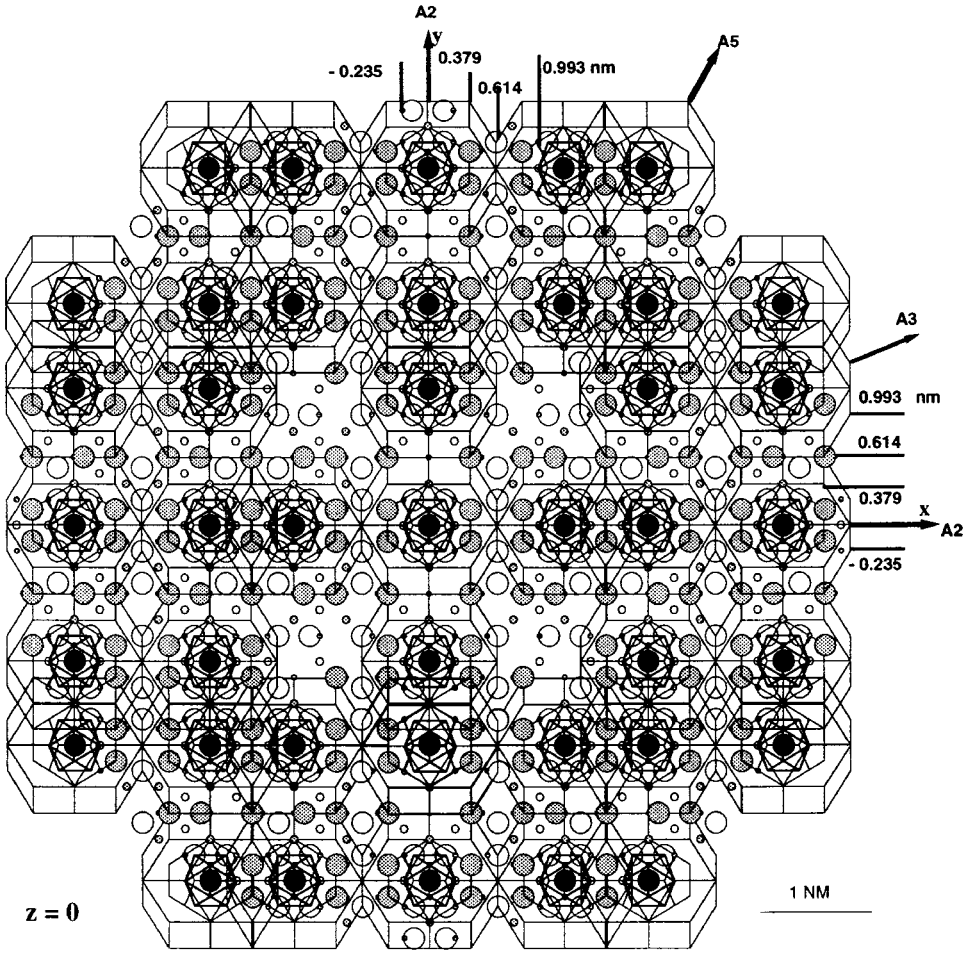

Fig. 3. Two-fold section of a 3D volume of icosahedral structure centred by a BC ● node. The largest circles are BC ●, N′ ◌ and N ○ nodes of the three occupied sublattices, located in the section $z = 0$; the smaller circles are projections of nodes located in a slice of thickness $z = \pm 0.332$ nm. Each two-fold axis bears nodes belonging to only one sublattice; this allows a simple description of the cubic cells.

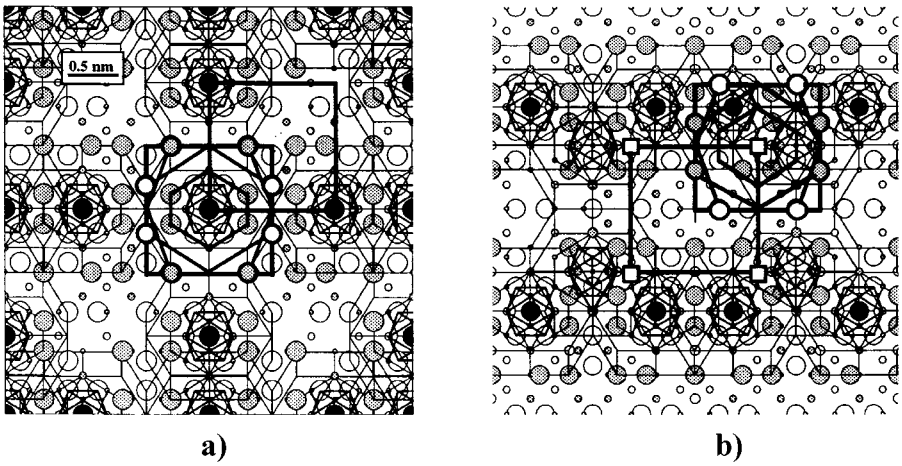

Fig. 4. Structure of cubic cells constructed on BC ● and unoccupied BC′ □ nodes as vertices and centre: (a) in the section $z = 0$; (b) in the section $z = \pm 1/2a_\alpha$. In both cells there is a triacontahedron inscribed in the cell: icosahedron on N′ ◌ nodes and dodecahedron on N ○ nodes in Figure 5a and reciprocally in Figure 5b. The cluster surrounding the BC ● nodes is a Bergman cluster; a slightly modified Bergman cluster surrounds the BC′ node.

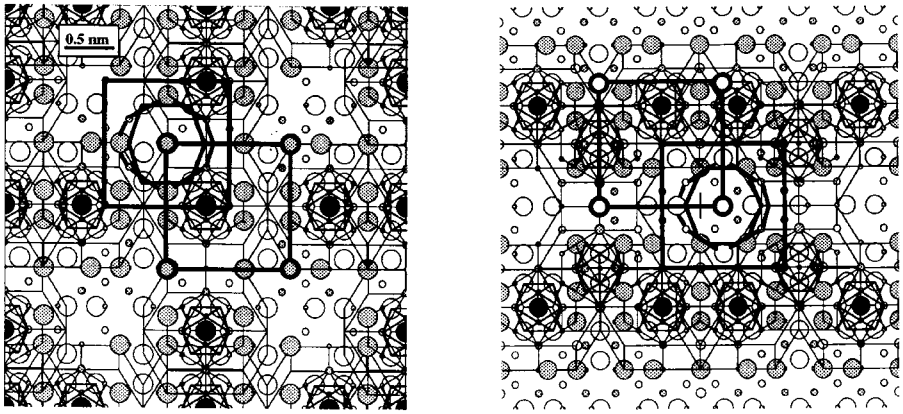

Fig. 5. Structure of cubic cells constructed on N ○ and N′ ◎ nodes as vertices and centre: (a) in the section $z = 0$; (b) in the section $z = \pm 1/2a_\alpha$. Only some nodes of the triacontahedron inscribed in the cell are occupied by BC ● nodes. The cluster surrounding the N/N′ vertices and centre are "pseudo-Mackay" clusters.

to the orbits of the Bergman cluster [13] that surround the BC centre (icosahedron of radius $a_{\rm ico}/\tau$ on N nodes and dodecahedron of radius $0.910a_{\rm ico}$ on N′ nodes and reciprocally in Fig. 4b). This description of the cell presents similarities with the description of the R Al_5CuLi_3 1/1 approximant cell [14,15], and with the structure of the 1/1 cubic AlPdMn approximant cell [16].

In the same way, Figures 5a and 5b represent cubic cells constructed on N and N′ nodes as vertices and centre. The clusters surrounding these vertices and centre are pseudo-Mackay clusters [15,17]: small dodecahedron of radius $0.910/\tau a_{\rm ico}$ (partially occupied), icosahedron of radius $a_{\rm ico}$, icosidodecahedron of radius $1.05a_{\rm ico}$. These cells present similarities with the cell of the αAlMnSi 1/1 approximant [18–21].

However, in the α(AlSi)CuFe cell there is an important difference which results from the occupied nodes of the BC sublattice. The 64 BC and BC′ nodes of a 6D unit cell belonging to P_2 project on 3D atomic sites located on orbits identical to those of P_1; however while the nodes of the N and N′ sublattices are fully occupied (the smallest distance along a two-fold axis, equal to 0.290 nm, is in the range of interatomic distances), the BC sublattice is only partially occupied (smallest distance along a two-fold axis = 0.759 nm). (The vacant nodes of the BC′ sublattice are not represented on the sections of the icosahedral structure). The occupied nodes of the BC sublattice (always surrounded by a Bergman cluster) are located on the triacontahedron inscribed in the cell: they are on the icosahedron in a cell centred by a N′ node (Fig. 5a) and on the dodecahedron in a cell centred by a N node (Fig. 5b). Their distribution on these orbits obeys the different local symmetries of the icosahedral structure; thus the number and the localisation of the occupied BC nodes can be different from a cell to the next one. Despite this asymmetric occupation of the four sublattices, we define hereafter a general description of the 1/1 cubic approximant cell:

- we select in the AlCuFe icosahedral model the cells constructed on N/N′ vertices; the large number of pseudo-Mackay clusters allows the identification of such cells everywhere;
- we retain as convenient cells, only those in which the occupied BC nodes are localised on the icosahedron (or the dodecahedron) inscribed in the cell; thus there is no disorder in the cell. However, their localisation on these orbits can be different from one cell to another. This can be considered as a partial occupation of the sites on the orbits.

This restrictive definition of the cell allows the identification, in the icosahedral structure, of different domains formed by a few "periodic" cells.

3.2 Domains of periodic cells in the AlCuFe icosahedral structure

We described [5] in a 3D model of the icosahedral structure, large concentric orbits surrounding a local symmetry centre. Here, there are around the BC centre (Fig. 6a), a large icosahedron (12 N nodes, 20 faces in three-fold planes) and a large dodecahedron (20 N′ nodes, 12 faces in five-fold planes) whose edge length is equal to the edge length a_α of the 1/1 cubic unit cell.

In this section ($z = 0$) of the icosahedral model, we have drawn a small domain of periodic cells constructed on N′ vertices. The faces of these cells correspond to the face represented in Figure 5a; the occupied BC nodes are on the dodecahedron inscribed in the cell and their localisation on this orbit is different in the cells belonging to the domain.

One can see that the edge parallel to y of the large dodecahedron (shown by largest N′ circles in Fig. 6a) belongs to this small domain of periodic cells. The ($z = 0$) two-fold plane being a mirror plane of the icosahedral structure, this edge is shared by 4 cells on N′ vertices. Figure 6b, in the section $z = \pm 1/2a_\alpha = \pm 0.614$ nm, represents the cells of the same domain, constructed on the N vertices located at the centre of the preceding cells; their faces

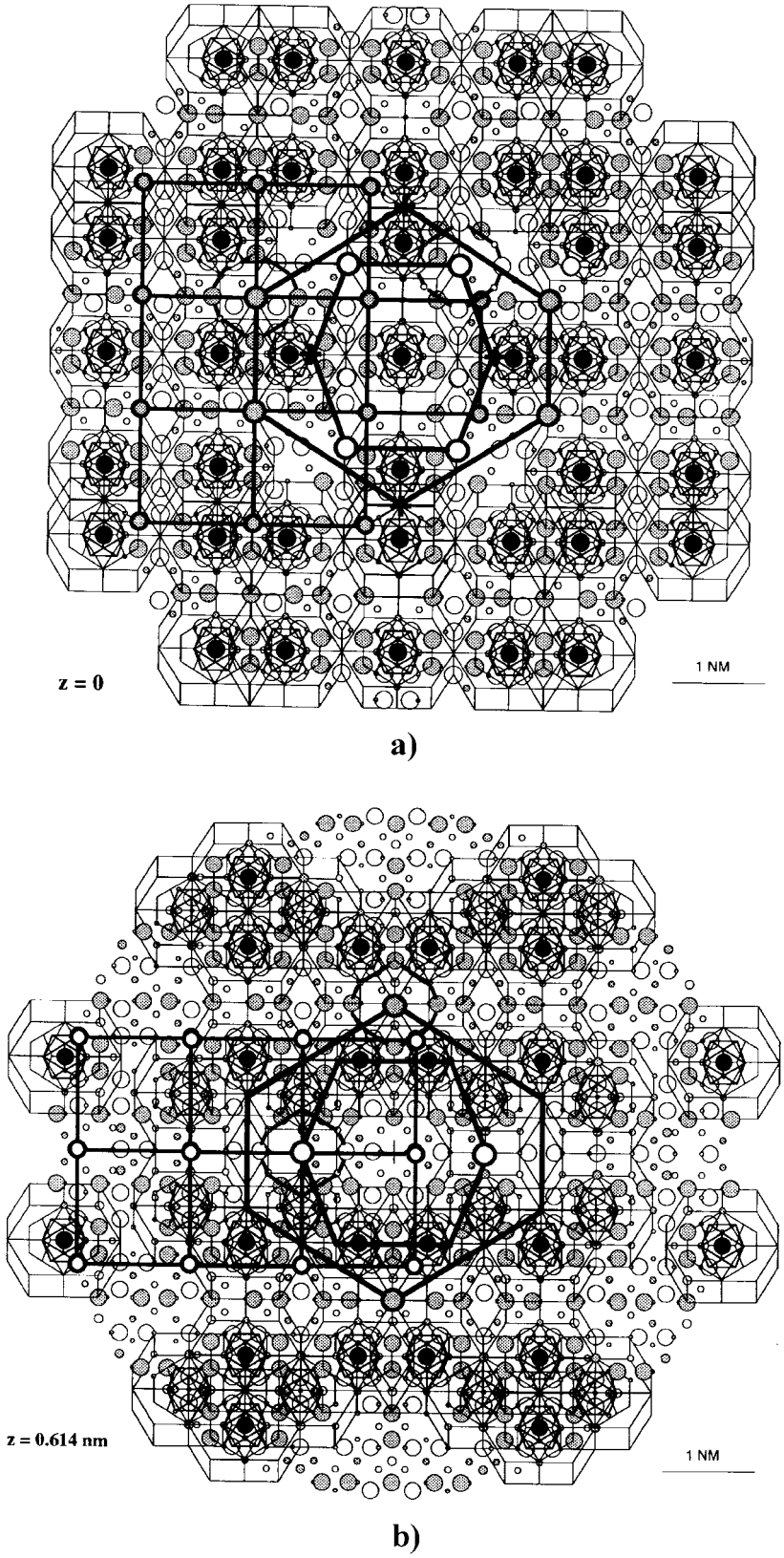

Fig. 6. Identification of a domain of periodic cells in two different sections of the icosahedral model: (a) in the section $z = 0$ the domain is linked to a dodecahedron edge parallel to y, shown by larger N′ ● circles; (b) in the section $z = \pm 1/2a_\alpha$ the same domain is linked to an icosahedron edge parallel to z, shown by a larger N ○ circle.

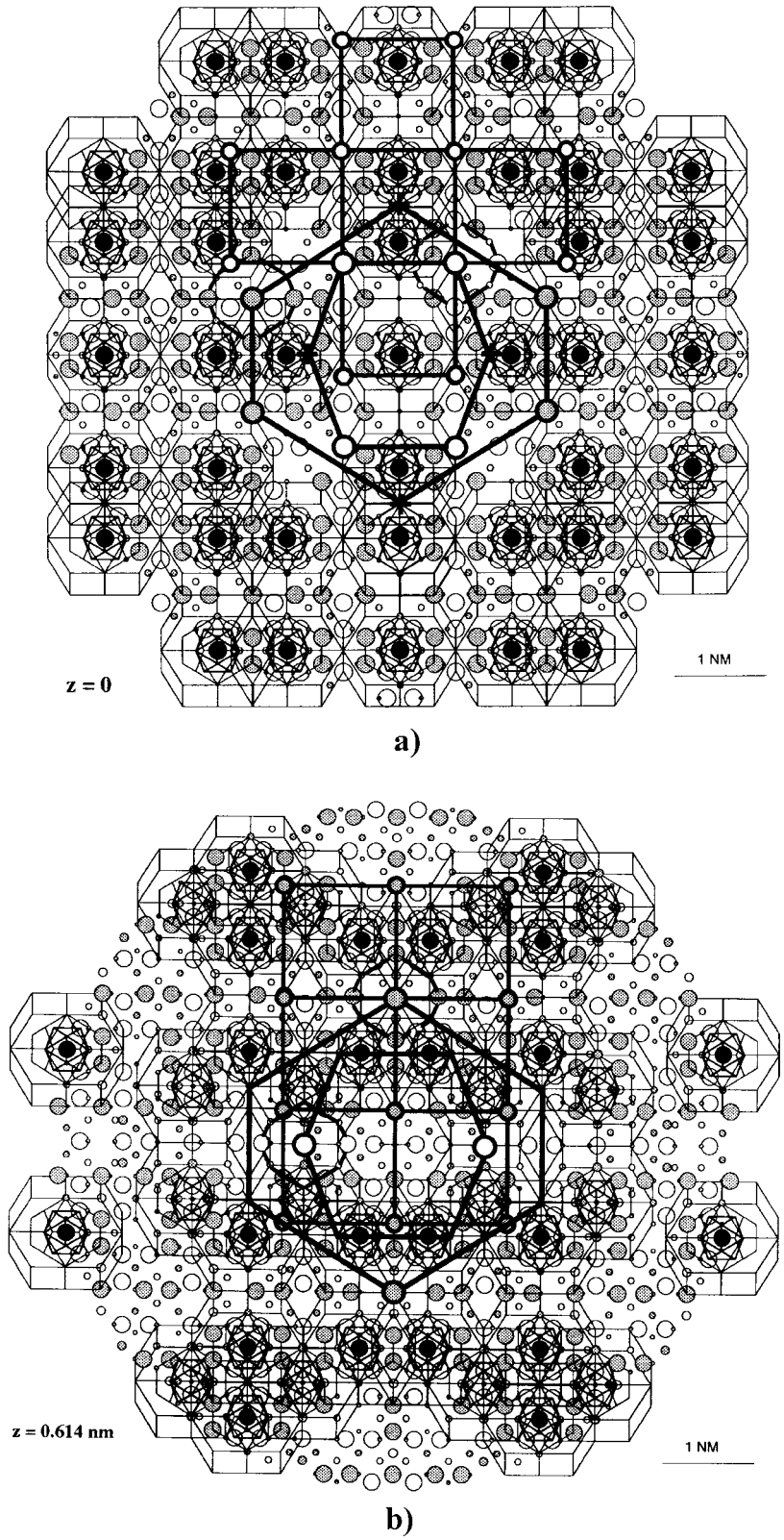

Fig. 7. Determination of another domain of periodic cells in the same sections of the icosahedral model: (a) in $z = 0$ the domain is linked to an icosahedron edge parallel to x (larger N ○ circles); (b) in $z = \pm 1/2a_\alpha = \pm 0.614$ nm it is linked to a dodecahedron edge parallel to z, shown by a larger N′ ◎ circle.

correspond to the face represented in Figure 5b (in this case, the occupied BC nodes are on the icosahedron inscribed in the cell). The edge parallel to z of the large icosahedron (shown by the largest N circle) is shared by four cells on N vertices. Thus this domain is linked to both a dodecahedron edge and an icosahedron edge respectively perpendicular one to another.

The limits of the domain are not well defined. Within the cells, the Bergman and pseudo-Mackay clusters either share a five-fold face (in a cell on N′ vertices) or a three-fold plane (in a cell on N vertices). On the borders of the domains, the vertices of the cells are close to the Bergman clusters located outside the domain: either the pseudo-Mackay cluster cannot be complete, or a local reconstruction may occur.

Figure 7 represents another domain linked to an icosahedron edge parallel to x in the section $z = 0$ (Fig. 7a), and to a dodecahedron edge parallel to z in the section $z = \pm 1/2 a_\alpha = \pm 0.614$ nm (Fig. 7b).

A third domain of cells (not represented here) corresponds to the association of an icosahedron edge parallel to y in the section $z = 1/2 a_\alpha + 0.379$ nm $= 0.993$ nm, and a dodecahedron edge parallel to x in the section $z = a_\alpha + 0.379$ nm.

These 3 domains and those symmetric with respect to the three orthogonal two-fold planes, are thus related to the 12 N nodes of the large icosahedron and to 12 over the 20 N′ nodes of the large dodecahedron.

The set of translation vectors between these 6 domains can be easily determined (Fig. 8a): the 12 N nodes of the large icosahedron and 12 over the 20 N′ nodes of the large dodecahedron are linked by vectors of length a_α (or a multiple of a_α) to N′ and N nodes of the triacontahedron surrounding the BC centre. The smallest translation vector between two of these domains is equal to the edge of the triacontahedron, which is a vector of length $a_{\mathrm{ico}} = 0.4465$ nm along a five-fold axis, joining N and N′ nodes.

The 8 remaining N′ nodes of the dodecahedron, of coordinates $x = y = z = 0.993$ nm, are on a cube of edges parallel to x, y and z. They correspond to 8 more domains. Along each diagonal of the cube (Fig. 8b), which is also an icosahedral three-fold axis, there are three nodes belonging to the same domain: N′ ($x = y = z = 0.993$ nm) on the large dodecahedron; N′ ($x = y = z = -0.235$ nm) on a very small cube inscribed in the central Bergman cluster; and, at the centre of the cell, a N node ($x = y = z =$ 0.379 nm) which is located on the triacontahedron. The length of the N to N′ translation vector, between opposite domains on the same diagonal, is 0.251 nm along a three-fold axis (the two-fold projections of this vector along the x, y, and z axis are only 0.145 nm). Figure 8c collects the locations of all these nodes on a two-fold projection of the triacontahedron.

Thus, in the volume of icosahedral structure here considered, $((3\times 2)+8) = 14$ different but equivalent domains of a few periodic cells can be identified.

3.3 HREM images of the α $Al_{55}Si_7Cu_{25.5}Fe_{12.5}$ cubic approximant phase

The observation of various samples of the α $Al_{55}Si_7Cu_{25.5}Fe_{12.5}$ phase leads to the following remarks. The definition of the HREM image is better in the cases where elements of the icosahedral structure can be observed: diffuse traces of planes parallel to icosahedral five-fold planes, or identification of the two-fold projection of the nodes of a triacontadron inscribed in each cell (as in Figs. 2c and 2d).

The BC′ sublattice being vacant in the AlCuFe icosahedral structure, this triacontahedron corresponds necessarily to an icosahedron on N′ nodes and a dodecahedron on N nodes as in Figure 4a (or reciprocally as in Fig. 4b). The simplest hypothesis would be that this contrast corresponds to the internal structure of a cell similar to the R Al_5CuLi_3 cell (Fig. 4a). However, the BC centres of the cells, occupied in the AlCuFe icosahedral phase by Cu atoms surrounded by a Bergmann cluster, are not apparent on these images; there is no evidence for a symmetry centre. On the contrary, one can identify the four dots of coordinates $x = y = z = \pm 0.235$ nm located on the Bergman cluster in Figure 8b.

Thus the contrast observed within the cells corresponds better to Figure 8c which reveals the superposition of different domains of periodic cells in the icosahedral structure, than to the structure of the cell represented in Figure 4a.

These observations lead us to the hypothesis that the cubic approximant structure could result from the superposition of domains "inherited" from the "parent" icosahedral structure. The number and nature of the preserved domains can be different in various parts of a sample; that would explain some surprising results, incompatible with the concept of periodic arrangement of identical cells: particularly, the variation (Fig. 2d) from one cell to the next, of the relative intensities of a group of 3, 4 or 5 dots brighter than the others.

A similar "square" group of intense dots is apparent too in Figure 2b, taken out of the same sample; in this case, there are no traces of five-fold planes and the triacontahedron cannot be identified; the structure seems perfectly periodic but the dots are less sharp.

It cannot be said if the differences between these three kinds of images result from the number and nature of the domains of periodic cells through the thickness of the sample or if they correspond to different stages of the transformation into the cubic structure.

3.4 Translation defects in the α $Al_{55}Si_7Cu_{25.5}Fe_{12.5}$ cubic approximant phase

Figure 9a is an example of translation defects between domains issued from different regions of the "parent" icosahedral phase.

– The contrast observed within the cells is the same on both sides of the boundary, so we suppose that there is no rigid-body translation along the z axis.

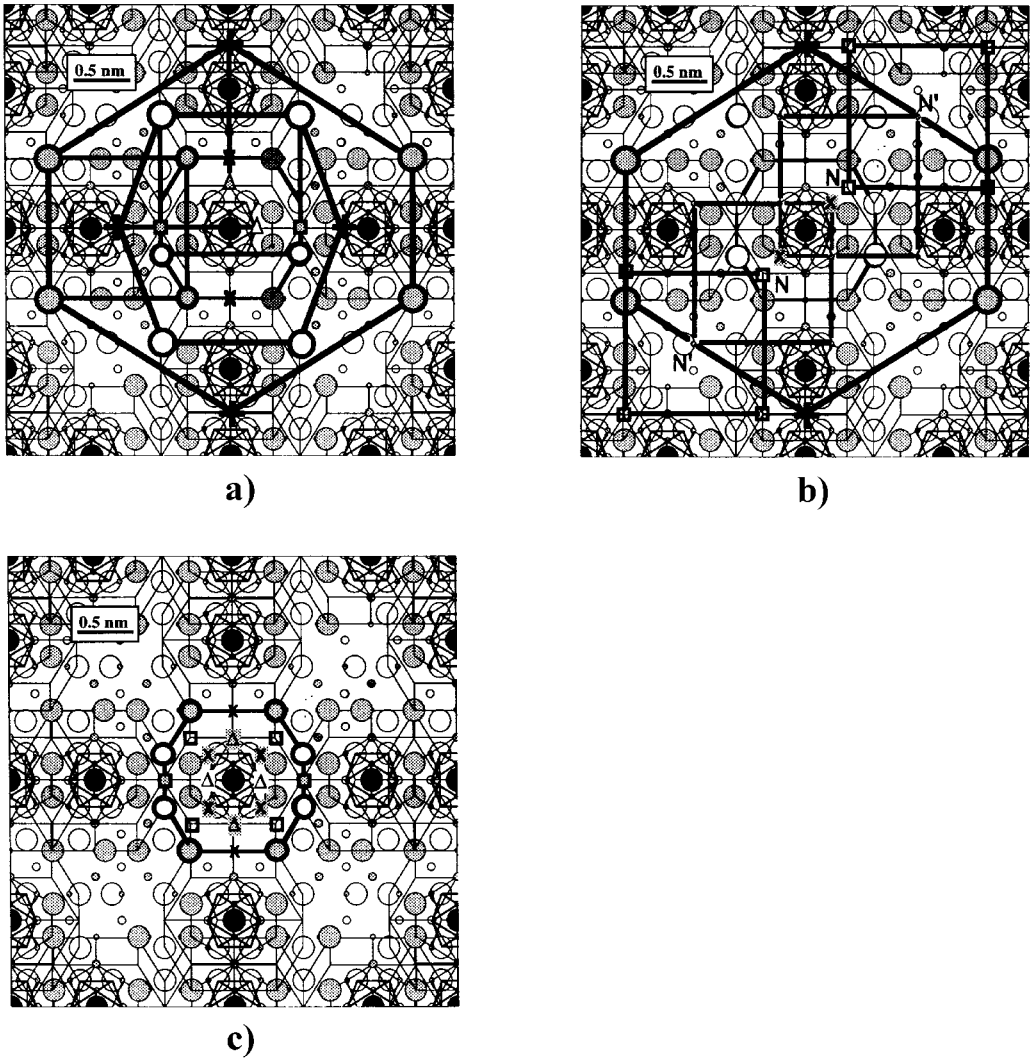

Fig. 8. Translation vectors between the different domains of periodic cells. (a) The 6 domains linked to edges of the large icosahedron and the large dodecahedron are related by vectors of length a_α to N/N′ nodes of a triacontahedron surrounding the BC centre. The smallest translation vector between them is equal to the edge of this triacontahedron (0.4465 nm along a five-fold axis). (b) The 8 remaining domains are linked to the N′ vertices of the large dodecahedron which form a cube; along a diagonal of this cube there are three nodes within a cell: N′ ($x = y = z = 0.993$ nm) on the large dodecahedron; N′ ($x = y = z = -0.235$ nm) on a very small cube inscribed in the central Bergman cluster; and, at the centre of the cell, a N node ($x = y = z = 0.379$ nm) which is located on the triacontahedron. The N to N′ translation vector between opposite domains on a same diagonal is 0.251 nm along a three-fold axis. (c) Two-fold projection of the translations between the 14 domains. ● ○ in $z = 0$; ⊠ ⊡ nodes in $z = \pm 0.235$ nm $= \pm(0.993 - 1.228$ nm); ■ □ nodes in $z = \pm 0.379$ nm; ▲ △ nodes in $z = \pm 0.614$ nm.

- Both domains are separated by the translation defect in such a way that the traces of the (110) and $(\bar{3}10)$ planes are not misaligned through the boundary. (One can observe at glancing angle the misalignment of the traces of the $(\bar{1}10)$, (100) and (010) planes.)
- The measure, by geometric phase analysis of the rigid body translation components along the x and y axes leads to a vector whose length and orientation are nearly $a_{\rm ico} = 0.4465$ nm along a five-fold axis. This translation vector may correspond to any one of the N → N′ translations between different domains of periodic cells: for example, in the section $z = 0$, the domains drawn respectively, on N′ nodes (Fig. 6a) and N nodes (Fig. 7a), or in the section $z = 1/2a_\alpha = 0.614$ nm, the domains drawn respectively on N nodes (Fig. 6b) and N′ nodes (Fig. 7b).

We have superposed in Figure 9b, the domains on N and N′ nodes represented in the section $z = 0$ (Figs. 6a and 7a). It appears that the N and N′ traces of the (110) plane and $(\bar{3}10)$ plane are very close one by another but not exactly superposed. Their superposition could be achieved by a small additional translation which may explain the diffuse streaks parallel to the traces of five-fold planes in Figure 9a.

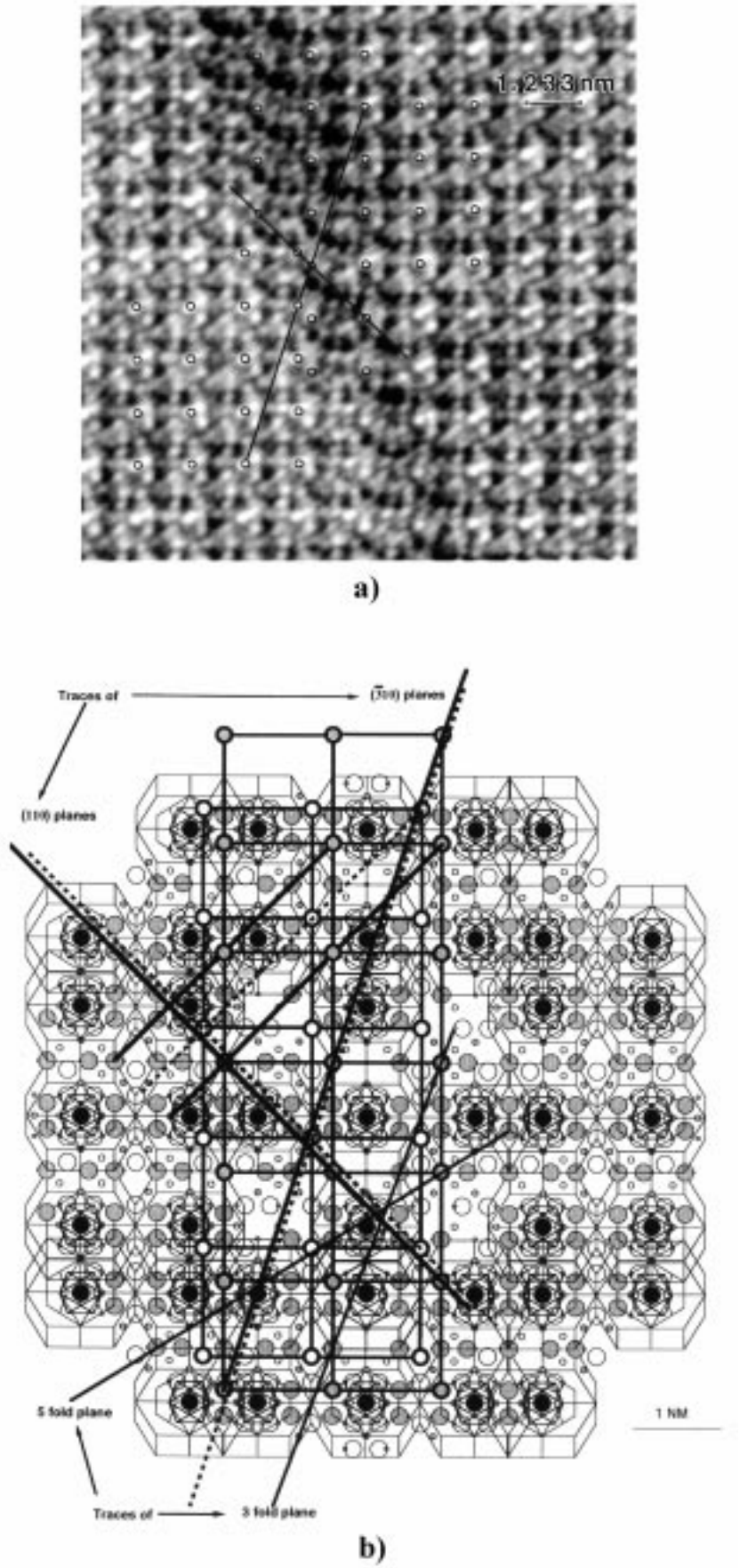

Fig. 9. Translation defect in the $\alpha Al_{55}Si_7Cu_{25.5}Fe_{12.5}$ cubic approximant phase. (a) The traces of the (110) and $(\overline{3}10)$ planes are not misaligned through the boundary. The translation vector measured by geometric phase analysis, is nearly equal to $a_{\mathrm{ico}} = 0.4465$ nm along a five-fold axis. (b) Superposition of 2 domains of periodic cells on N ○ and N′ ● nodes, translated one from another by this vector; the traces of the (110) and $(\overline{3}10)$ planes corresponding to each domain are not exactly superposed.

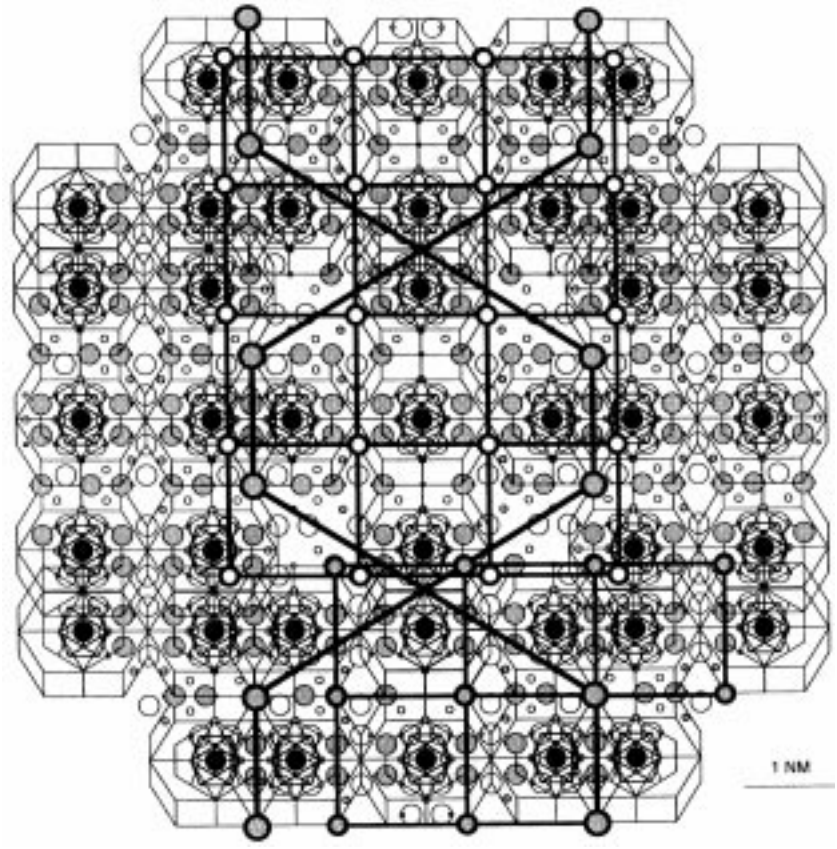

Fig. 10. Junction between 2 domains of periodic cells on N ○ and N′ ● nodes issued from different dodecahedra of the icosahedral structure. The domain drawn on N nodes is equivalent to the domain shown in Figure 7a; the domain drawn on N′ nodes is equivalent to the domain shown in Figure 6a. The two-fold components of the translation vector of length 0.251 nm, along a three-fold axis, are $x = 0.145$ nm, $y = 0.9$ nm and $z = 0$.

Thus, small rearrangements within the structure could improve the perfection of a cubic phase resulting from a selection of different domains in the icosahedral phase. Such a process rather corresponds to a displacive transformation than to a reconstructive transformation.

3.5 Structural transformation from the icosahedral to the cubic approximant structure

The icosahedral structure can be described as an aperiodic distribution of dodecahedra of edge a_α, identical to the dodecahedron used in Figure 8 to describe the different domains.

The growth of any nucleus of cubic structure from only one dodecahedron would need the reconstruction of the whole icosahedral structure. This seems to be unlikely; it is in contradiction with the stability attributed to the Bergman clusters and with the rapidity of transformation of the icosahedral (AlSi)CuFe phase into the cubic phase, as reported by Quivy *et al.* [1]. We rather propose that domains of a few cubic cells, issued from different dodecahedra, could join together in such a way as to construct a periodic structure. In this hypothesis, the Bergman clusters are already at their convenient places in the domains; however, the extension of the periodic structure needs a partial reconstruction between joining domains, and, in any case, a translation vector exists between the domains.

The translation defects which are easily detected by HREM (Fig. 9) and [7,8] correspond to the large translation vectors which can be measured by geometric phase analysis. However, domains separated by smaller translation vectors can also participate in the structural transformation of the icosahedral phase. Figure 8b shows domains linked by a translation vector of length 0.251 nm, along a three-fold axis of the icosahedral structure which is also a $\langle 111 \rangle$ direction of the cube. The components of the translation vector in the $\{100\}$ planes are only 0.145 nm.

Figure 10 is a more general example of assemblage of domains: in this case the domains belong to two different dodecahedra of edge a_α. (The domain drawn on N nodes is equivalent to the domain shown in Fig. 7a; the domain drawn on N′ nodes is equivalent to the domain shown in Fig. 6a.) Both domains have in common the $\{100\}$ plane of the figure. The translation vector in this plane is 0.251 nm along a three-fold axis (its components are $x = 0.145$ nm, $y = 0.9$ nm, $z = 0$).

One may suppose that in both cases the corresponding translation defect between the domains either cannot be detected by HREM or disappears by relaxation during

the transformation process. These examples could explain why, on the HREM images of the α ($Al_{55}Si_7Cu_{25.5}Fe_{12.5}$) cubic approximant phase, one can observe large areas without apparent defect.

4 Conclusion

The study in a 3D model of AlCuFe icosahedral structure of the possibilities of transformation of an icosahedral structure into a periodic cubic structure leads to a model of transformation which could explain the unusual results obtained by High Resolution Electron Microscopy study of the α $Al_{55}Si_7Cu_{25.5}Fe_{12.5}$ 1/1 cubic approximant phase. This cubic structure could be described as the superposition of various domains of periodic cubic cells "inherited" from the "parent" icosahedral structure. The transformation would result from an assemblage of some of the domains, followed by slight rearrangements in the cubic structure.

We would like very much to thank Dr M. Hÿtch for helpful discussions.

References

1. A. Quivy, M. Quiquandon, Y. Calvayrac, F. Faudot, D. Gratias, C. Berger, R.A. Brand, V. Simonet, F. Hippert, J. Phys. Cond. Matter **8**, 4223 (1996).
2. M. Hÿtch, Microsc. Microanal Microstr. **8**, 41 (1997).
3. A. Katz, D. Gratias, J. Non Cryst. Solids **153-154**, 187 (1993).
4. A. Katz, D. Gratias, *Proc. ICQ5*, edited by C. Janot, R. Mosseri (World Scientific, 1995), p. 164.
5. A. Le Lann, J. Devaud, J. Phys. I France **5**, 129 (1995).
6. L. Bresson, A. Quivy, F. Faudot, M. Quiquandon, Y. Calvayrac, *Proc. ICQ6*, edited by S. Takeuchi, T. Fujiwara (World scientific, 1997), p. 211.
7. M. Quiquandon, D. Gratias, J. Devaud, A. Le Lann, M. Hÿtch, L. Bresson, A. Katz, *Proc. ICQ6*, edited by S. Takeuchi, T. Fujiwara (World scientific, 1997), p. 239.
8. A. Le Lann, M. Hÿtch, J. Devaud, *Proc. Aperiodic 97*, edited by M. de Boissieu, J.L. Verger-Gaugry, R. Currat (World Scientific, 1998), p. 229.
9. D. Gratias, A. Katz, M. Quiquandon, J. Phys. Cond. Matter **7**, 9101 (1995).
10. M. Cornier-Quiquandon, R. Bellissent, Y. Calvayrac, J.W. Cahn, D. Gratias, B. Mozer, J. Non Cryst. Solids **153-154**, 10 (1993).
11. A. Le Lann, Phil. Mag. B **66**, 653 (1992).
12. A. Le Lann, J. Devaud, *Proc. ICQ5*, edited by C. Janot, R. Mosseri (World Scientific, 1995), p. 672.
13. G. Bergman, L.T. Waugh, L. Pauling, Acta Cryst. **10**, 254 (1957).
14. M. Audier, P. Sainfort, B. Dubost, Phil. Mag. B **54**, L105 (1986).
15. N. Tamura, Phil. Mag. A **76**, 237 (1997).
16. K. Sugiyama, N. Kaji, K. Hiraga, T. Ishimasa, Z. Kristallogr. **213**, 168 (1998).
17. M. Boudard, M. de Boissieu, C. Janot, G. Heger, C. Beeli, H.U. Nissen, H. Vincent, R. Ibberson, M. Audier, J.M. Dubois, J. Phys. Cond. Matter **4**, 10149 (1992).
18. M. Cooper, K. Robinson, Acta Cryst. **20**, 614 (1966).
19. P. Guyot, M. Audier, Phil. Mag. B **52**, L15 (1985).
20. V. Elser, C.L. Henley, Phys. Rev. Lett. **55**, 2833 (1985).
21. H.D. Fowler, B. Mozer, J. Sims, Phys. Rev. B **37**, 3906 (1988).